Since January 2020 Elsevier has created a COVID-19 resource centre with free information in English and Mandarin on the novel coronavirus COVID-19. The COVID-19 resource centre is hosted on Elsevier Connect, the company's public news and information website.

Atmospheric Research 250 (2021) 105362

Contents lists available at ScienceDirect

Atmospheric Research

journal homepage: www.elsevier.com/locate/atmosres

COVID-19 pandemic in Wuhan: Ambient air quality and the relationships between criteria air pollutants and meteorological variables before, during, and after lockdown

Ishaq Dimeji Sulaymon [a], Yuanxun Zhang [a,b,*], Philip K. Hopke [c,d], Yang Zhang [a], Jinxi Hua [a], Xiaodong Mei [a]

[a] College of Resources and Environment, University of Chinese Academy of Sciences, Beijing 100049, China
[b] CAS Center for Excellence in Regional Atmospheric Environment, Chinese Academy of Sciences, Xiamen 361021, China
[c] Center for Air Resources Engineering and Science, Clarkson University, Potsdam, NY 13699, USA
[d] Department of Public Health Sciences, University of Rochester School of Medicine and Dentistry, Rochester, NY 14642, USA

ARTICLE INFO

Keywords:
COVID-19
Lockdown
Wuhan
Criteria air pollutants
Meteorological variables
HYSPLIT

ABSTRACT

As a result of the lockdown (LD) control measures enacted to curtail the COVID-19 pandemic in Wuhan, almost all non-essential human activities were halted beginning on January 23, 2020 when the total lockdown was implemented. In this study, changes in the concentrations of the six criteria air pollutants ($PM_{2.5}$, PM_{10}, SO_2, NO_2, CO, and O_3) in Wuhan were investigated before (January 1 to 23, 2020), during (January 24 to April 5, 2020), and after the COVID-19 lockdown (April 6 to June 20, 2020) periods. Also, the relationships between the air pollutants and meteorological variables during the three periods were investigated. The results showed that there was significant improvement in air quality during the lockdown. Compared to the pre-lockdown period, the concentrations of NO_2, $PM_{2.5}$, PM_{10}, and CO decreased by 50.6, 41.2, 33.1, and 16.6%, respectively, while O_3 increased by 149% during the lockdown. After the lockdown, the concentrations of $PM_{2.5}$, CO and SO_2 declined by an additional 19.6, 15.6, and 2.1%, respectively. However, NO_2, O_3, and PM_{10} increased by 55.5, 25.3, and 5.9%, respectively, compared to the lockdown period. Except for CO and SO_2, WS had negative correlations with the other pollutants during the three periods. RH was inversely related with all pollutants. Positive correlations were observed between temperature and the pollutants during the lockdown. Easterly winds were associated with peak $PM_{2.5}$ concentrations prior to the lockdown. The highest $PM_{2.5}$ concentrations were associated with southwesterly wind during the lockdown, and northwesterly winds coincided with the peak $PM_{2.5}$ concentrations after the lockdown. Although, COVID-19 pandemic had numerous negative effects on human health and the global economy, the reductions in air pollution and significant improvement in ambient air quality likely had substantial short-term health benefits. This study improves the understanding of the mechanisms that lead to air pollution under diverse meteorological conditions and suggest effective ways of reducing air pollution in Wuhan.

1. Introduction

Around the end of December 2019, an infectious disease that was later linked to the family of coronaviruses was discovered in Wuhan, Hubei Province, China (Muhammad et al., 2020; Wang et al., 2020). Severe acute respiratory syndrome coronavirus 2 (SARS-CoV-2) was subsequently named by the World Health Organization (WHO) as COVID-19 (Chen et al., 2020; Muhammad et al., 2020). In January 2020, a cluster of COVID-19 cases was confirmed in Wuhan by the Chinese government. However, it rapidly spread to the neighboring cities in Hubei province and beyond (Muhammad et al., 2020). To control the COVID-19 epidemic, a total lockdown in Wuhan was announced by the Chinese government on January 23 and in Hubei province on January 24. After several days, the lockdown was extended across China. The lockdown measures were implemented primarily to reduce large gatherings and thereby control the spread of the virus (China State Council, 2020; Wang et al., 2020). The lockdown in Wuhan was in place until April 6, 2020. During the lockdown period, the control measures included the shutting down of all public transportation systems, schools, businesses centers, parks, non-essential industries, restaurants, and

* Corresponding author at: College of Resources and Environment, University of Chinese Academy of Sciences, Beijing 100049, China.

https://doi.org/10.1016/j.atmosres.2020.105362
Received 6 September 2020; Received in revised form 6 November 2020; Accepted 10 November 2020
Available online 12 November 2020

entertainment houses. Globally, about 1,226,813 deaths had been linked with COVID-19 as of November 6th, 2020 (WHO, 2020).

Criteria air pollutants ($PM_{2.5}$, PM_{10}, SO_2, NO_2, CO, and O_3) have serious effects on human health (GBD, 2020; USEPA, 2019). The adverse health outcomes range from increased emergency department visits, hospitalizations, and death from a variety of cardiorespiratory diseases. The WHO estimates that globally, there are 4.2 million premature deaths per year attributed to air pollution (https://www.who.int/airpollution/ambient/health-impacts/en/). For instance, epidemiological studies have identified significant associations between elevated airborne fine particulate matter ($PM_{2.5}$) concentrations and acute adverse health effects (e.g., Ayuni et al., 2014; Pope and Dockery, 2006; Sulaymon et al., 2017, 2018, 2020; Zhang et al., 2018). A positive association has been documented between ambient $PM_{2.5}$ concentrations and a variety of cardiovascular and respiratory health endpoints, including mortality, hospital admissions, emergency department visits, other medical visits, respiratory illness and symptoms, and physiologic changes in pulmonary function (e.g., Ayuni et al., 2014; Pope and Dockery, 2006; Zhang et al., 2018; Croft et al., 2018; Hopke et al., 2019).

The major sources of NO_2 pollution globally and in particular in China are the sources related to human activities (anthropogenic sources). Previous studies have found the combustion of fossil fuels. The main source of electrical energy are coal-fired power plants that are a major source of NO_2 (Zhao et al., 2020). In 2019, motor vehicles emitted over six million tons of nitrogen oxides in China (Statistica, 2020). Also, NO_2 pollution could occur due to the combustion of biomass materials. However, less attention is given to it since such an act is strictly forbidden in Chinese cities and urban areas (Zhao et al., 2020). Since a positive significant correlation has been established between the pollution level of NO_2 and human population size (Lamsal et al., 2013), increasing population and traffic sources contribute to the NO_2 pollution level (Zhao et al., 2020). Existing studies have revealed that air pollution due to NO_2 could trigger the risks of several diseases such as asthma, respiratory disease, and cardiovascular disease and even increase the rate of mortality due to the diseases (He et al., 2020; Lu et al., 2020a; Zhao et al., 2020). Brønnum-Hansen et al. (2018) reported that life expectancy of people residing in cities and urban areas could be elongated by an additional two years if the NO_2 concentration were reduced to same low level as in rural areas with low populations and vehicular movement.

In this study, changes in the concentrations of the six criteria air pollutants before, during, and after the 2020 COVID-19 lockdown period were investigated. Additionally, the pollutants concentrations during the same lockdown period in the prior three years were assessed. Also, the relationships between the air pollutants ($PM_{2.5}$, PM_{10}, SO_2, NO_2, CO and O_3) and four meteorological variables (temperature, wind speed, wind direction, and relative humidity) during the three periods were investigated using correlation analysis. This would improve the understanding of the mechanisms that lead to air pollution under diverse meteorological conditions and suggest potent ways of reducing air pollution in Wuhan. Furthermore, correlation analyses between the six criteria air pollutants during the three periods were performed to help ascertain the sources of emissions responsible for the reduction in concentrations of air pollutants during the periods. There is a lot of work on air quality during the COVID-19 lockdown period being reported from around the world (e.g., Chen et al., 2020; Mahato et al., 2020; Muhammad et al., 2020; Sharma et al., 2020; Wang et al., 2020). In Wuhan, there have been prior reports such as Lian et al. (2020). However, that study focused only on the pre-lockdown and during the lockdown periods and primarily on changes in the air quality index (AQI) rather than on the distributions of the various pollutants. This work is the first study to assess the relationships between the concentrations of the six criteria pollutants and the meteorological variables before, during, and after the COVID-19 pandemic lockdown period in Wuhan. These results would help identify effective control measures in mitigating air pollution in Wuhan and China as a whole especially during winter season.

2. Experimental methods

2.1. Study area and periods of study

The city of Wuhan (the capital of Hubei Province and the epicenter of COVID-19 in mainland China) was the focus of this study. The ambient concentrations of the six criteria air pollutants ($PM_{2.5}$, PM_{10}, SO_2, NO_2, CO, and O_3) prior to, during, and after the COVID-19 lockdown control measures were enacted and enforced in Wuhan by the Chinese government were compared. The pre-lockdown period was from January 1st to January 23rd, 2020, the lockdown (COVID-19 control) period ranged from January 24th through April 5th while the post-lockdown period was from April 6th through June 20th, 2020.

2.2. Data sources

Observations data from the eleven air quality monitoring stations covering this provincial capital city were used. One-hour data for particulate matter ($PM_{2.5}$ and PM_{10}), sulfur dioxide (SO_2), nitrogen dioxide (NO_2), ozone (O_3), and carbon monoxide (CO) were downloaded from the China's National Environmental Monitoring Center (http://www.cnemc.cn). The data have been validated (Wang et al., 2020; Zhao et al., 2019). The citywide daily mean concentrations were estimated by averaging the concentrations at the eleven air quality monitoring stations in Wuhan. In reporting the 24-hr average concentrations of the six criteria air pollutants to the public, the Chinese Ministry of Environmental Protection (MEP) uses this same method (Hu et al., 2015). Meteorological data were downloaded from the National Data Center of the Chinese Meteorological Agency (http://data.cma.cn).

2.3. Statistical analysis of the LD control measure

To study the impacts of the lockdown (LD) measures on air quality in Wuhan, the six criteria air pollutants were examined during the three consecutive periods; Pre-LD (January 1st - 23rd, 2020), During-LD (January 24th - April 5th, 2020) and Post-LD (April 6th - June 20th, 2020). To ascertain if the LD control measures resulted in reduction of observed concentrations of the pollutants, the data for the Pre-LD, During-LD, and Post-LD periods were compared using non-parametric statistical methods since the hourly concentrations were not normally distributed based on Shapiro-Wilk tests. For each air pollutant, the Kruskal-Wallis One Way Analysis of Variance (ANOVA) on Ranks (Kruskal and Wallis, 1952) among Pre-, During-, and Post-LD was performed with pairwise comparison using Dunn's method (Dunn, 1964). In addition, the 1-hr concentrations of the pollutants for the same lockdown period (i.e. January 24th - April 5th) for each of the last four years (2017–2020) were compared using the Kruskal-Wallis One Way Analysis of Variance (ANOVA) on Ranks and Dunn's tests (Tiwari et al., 2018). These analyses were conducted to assess the changes in pollutant concentrations over these years and to account for the changing photoperiod and temperatures that occur between January and June each year.

2.4. Relationships between air pollutants and meteorological variables

In order to investigate the relationships between the six air pollutants ($PM_{2.5}$, PM_{10}, SO_2, NO_2, CO and O_3) and the three meteorological variables (temperature, wind speed, and relative humidity), Pearson correlation analysis was conducted for the three study periods using SigmaPlot software (version 14). In addition, the relationship between the concentrations of the pollutants and their corresponding wind directions was investigated. The wind directions were categorized as follows: $337.5^\circ < N \leq 22.5^\circ$, $22.5^\circ <$ NE $\leq 67.5^\circ$, $67.5^\circ <$ E $\leq 112.5^\circ$, $112.5^\circ <$ SE $\leq 157.5^\circ$, $157.5^\circ <$ S $\leq 202.5^\circ$, $202.5^\circ <$ SW $\leq 247.5^\circ$,

247.5° < W ≤ 292.5°, 292.5° < NW ≤ 337.5°.

2.5. Backward trajectory model analysis

The trajectories with similar geographical origins were classified by computing the air mass backward trajectories (Khuzestani et al., 2017; Sulaymon et al., 2020). The calculations of the air mass backward trajectories were achieved using hybrid single-particle Lagrangian integrated trajectory model (HYSPLIT 4.9 version). In this study, the Global Data Assimilation System (GDAS) one-degree archive which has been used by the National Center for Environmental Prediction (NCEP) Global Forecast System (GFS) model was used. The computation of five-day backward trajectories with hourly interval and arrival height of 500 m above ground level (AGL) at the sampling sites was carried out using a vertical velocity model and 6 h interval between each starting time at every 24 h (Sulaymon et al., 2020).

3. Results and discussions

3.1. Changes in meteorological variables during the three periods

The daily average temperature, wind speed (WS), wind direction (WD), and relative humidity (RH) from January 1st, 2020, to June 20th, 2020 are presented in Fig. 1. During the Pre-LD period, temperatures were lower compared to During-LD period with the highest temperatures being recorded during the Post-LD period. A similar pattern was noted for WS. However, WD in the During-LD period had more frequent winds from the northeast (0–90°). The Post-LD period in terms of WS was relatively calm with highly variable wind directions. The highest and most stable RH values were observed during the Pre-LD period compared to the other two periods that had fluctuating RH values. The mean and standard deviation of temperature, WS, and RH were 11.2 ± 4.9 °C, 2.4 ± 0.9 m/s, and 75.1 ± 13.1%, respectively (Table 1). The most common WD across the three periods was north-easterly (0–90°).

The daily meteorological variable values from 2017 to 2019 (Figs. S1-S3) were also compared to the present year (i.e. 2020) during the lockdown period (Table 1). The average WD was southeasterly throughout with no significant changes in values between 2017, 2019, and 2020. This trend was also found in other variables except that the mean temperature in 2020 was somewhat higher than in the previous years. Thus, there was no significant differences for the meteorological variables among the years.

3.2. Changes in pollutant concentrations before, during, and after the lockdown period

The statistical analyses for the air pollutants during each of the three periods are summarized in Table 2. The detailed results are presented in Tables S1-S6. Daily mean $PM_{2.5}$, PM_{10}, SO_2, NO_2, CO and O_3 are shown

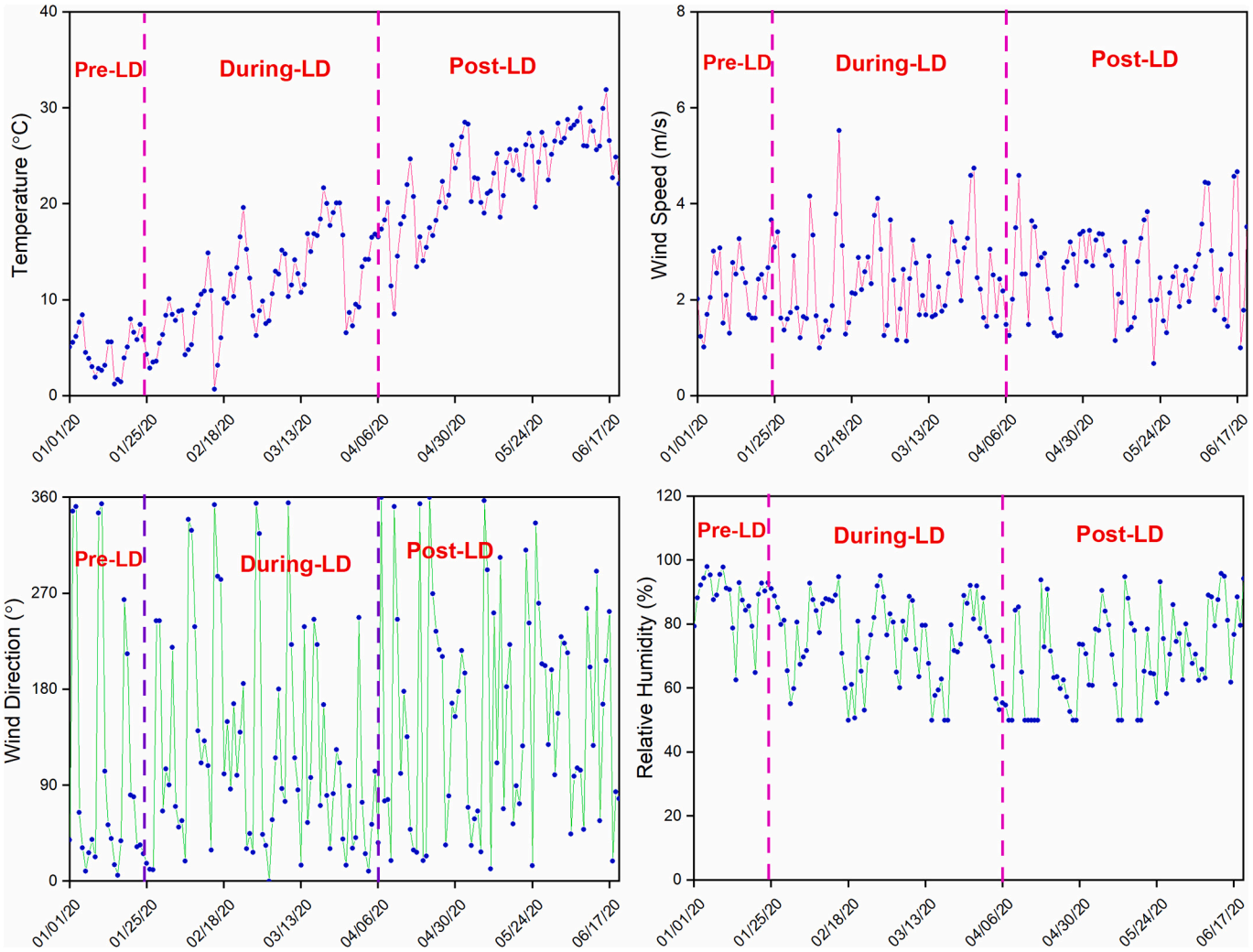

Fig. 1. Time series of daily average meteorological variables (temperature, wind speed, wind direction, and relative humidity) before, during and after the 2020 lockdown period in Wuhan.

Table 1
Basic statistics for the meteorological variables During-LD period from 2017 to 2020.

Parameter	Unit	Mean	Std Dev.	Maximum	Minimum	Median
2017						
Temperature	°C	10.45	4.41	19.64	2.1	10.49
Wind speed	m/s	2.52	1.07	6.6	0.83	2.19
Wind direction	°	122.72	95.35	355.23	9.14	106.79
Relative humidity	%	74.2	15.63	98.7	50	75.22
2018						
Temperature	°C	10.24	6.84	24.56	−3.40	9.86
Wind speed	m/s	2.93	0.97	5.30	1.2	2.91
Wind direction	°	101.79	78.65	358.48	7.16	77.12
Relative humidity	%	73.1	14.64	93.80	50	72.97
2019						
Temperature	°C	9.24	5.35	20.49	−0.46	8.63
Wind speed	m/s	2.46	1.11	7.92	1	2.23
Wind direction	°	120.79	111.65	359.73	3.72	72.03
Relative humidity	%	78.36	13.75	97.80	50	78.81
2020						
Temperature	°C	11.2	4.85	21.65	0.69	10.56
Wind speed	m/s	2.41	0.96	5.52	1.0	2.22
Wind direction	°	122.2	99	354.6	0.06	90.2
Relative humidity	%	75.1	13.1	95.1	50	77.3

Table 2
Basic statistics for the air pollutants during Pre-LD, During-LD, and Post-LD periods.

Pollutant	Unit	Number	Mean	Std Dev.	Max	Min	Median
Pre-LD							
$PM_{2.5}$	$\mu g/m^3$	548	63.32	31.98	133	4	61
PM_{10}	$\mu g/m^3$	548	75.47	37.13	163	5	79
SO_2	$\mu g/m^3$	548	6.78	2.39	19	5	6
NO_2	$\mu g/m^3$	548	43.17	15.30	107	18	42
CO	mg/m^3	548	1.08	0.27	2.2	0.6	1.1
O_3	$\mu g/m^3$	548	25.13	18.51	92	4	23
Dur-LD							
$PM_{2.5}$	$\mu g/m^3$	1635	37.26	19.93	138	3	34
PM_{10}	$\mu g/m^3$	1635	50.46	26.27	160	5	47
SO_2	$\mu g/m^3$	1635	8.12	3.72	37	4	7
NO_2	$\mu g/m^3$	1635	21.34	8.90	59	7	19
CO	mg/m^3	1635	0.90	0.25	2.1	0.3	0.9
O_3	$\mu g/m^3$	1635	62.49	26.38	163	10	58
Post-LD							
$PM_{2.5}$	$\mu g/m^3$	1772	29.97	12.91	90	2	29
PM_{10}	$\mu g/m^3$	1772	53.42	24.02	141	3	50
SO_2	$\mu g/m^3$	1772	7.95	3.68	34	4	7
NO_2	$\mu g/m^3$	1772	33.19	20.29	115	8	27
CO	mg/m^3	1772	0.76	0.20	1.7	0.3	0.7
O_3	$\mu g/m^3$	1772	78.26	42.139	213	4	72

in Fig. 2. The median values of $PM_{2.5}$ decreased monotonically with significant differences between Pre-LD vs During-LD (61.0–34.0) and Pre-LD vs Post-LD (61.0–29.0) (Fig. 3). All of the pairwise differences were also significant. The Post-LD values were actually less than During-LD, although the difference (399) is much smaller than Pre-LD vs Post-LD with difference of 1291 (Table S1). A larger difference of ranks (892) was observed between Pre-LD vs During-LD.

The differences in the median values of PM_{10} between the three periods are statistically significant (Table 3). The median values of PM_{10} declined with significant differences between Pre-LD vs During-LD (79.0–47.0) and Pre-LD vs Post-LD (79.0–50.0) (Fig. 3). PM_{10} is different from $PM_{2.5}$ with Post-LD > During-LD. The Dunn's test (Table S2) showed that all of the pairwise differences were significant. Contrary to $PM_{2.5}$, Post-LD is greater than During-LD, although the difference (152) is small compared to that of Pre-LD vs During-LD and Pre-LD vs Post-LD whose differences were 822 and 670, respectively. The slight difference between the median values of Post-LD vs During-LD was due to the ease of lockdown as life activities returned to normal in Wuhan.

The ANOVA on ranks showed that there exists a statistically significant difference in the median values of SO_2 (Table 2). Contrary to $PM_{2.5}$ and PM_{10}, the median values of SO_2 increased with significant differences between Pre-LD vs During-LD (6.0–7.0) and Pre-LD vs Post-LD (6.0–7.0) (Table 2). According to the Dunn's test (Table S3), only two of the pairwise differences were found to be statistically significant. During-LD is only slightly greater than Post-LD with difference of ranks (17.8) and insignificant. During-LD vs Pre-LD (459) and Post-LD vs Pre-LD (441) were significantly different. The significant difference between median values of During-LD vs Pre-LD is an indication that the concentration of SO_2 increased despite the lockdown measures. The rise in the concentration of SO_2 during the lockdown period may be attributed to additional coal heating activities during the winter season since people stayed at home so there was more need for heating and cooking. SO_2 is a major pollutant from residential coal combustion.

NO_2 behaved similarly to PM_{10}. The differences in the median values among the three periods were found to be statistically significant. The median values of NO_2 substantially declined between Pre-LD vs During-LD (42.0–19.0) and Pre-LD vs Post-LD (42.0–27.0). An increase in the median value for the Post-LD was observed just as in the case of PM_{10}. Considering the Dunn's test (Table S4), all of the pairwise differences were significant. The highest difference of ranks (1608) was observed between Pre-LD vs During-LD, a reflection of what was observed in the Kruskal-Wallis' test. Pre-LD vs Post-LD and Post-LD vs During-LD had difference of ranks of 853 and 755, respectively. The significant reduction (~50%) in NO_2 during the lockdown period showed that vehicular traffic is a major source of air pollution in Wuhan. The increase in concentrations was observed as the lockdown was relaxed and vehicular movement resumed.

CO behaved similarly to $PM_{2.5}$. The median values declined monotonically with significant differences between Pre-LD vs Post-LD (1.10–0.70) and Pre-LD vs During-LD (1.10–0.90). All the pairwise differences were also statistically significant. Pre-LD is greater than Post-LD (1336). A significant difference of ranks (703) was observed between Pre-LD vs During-LD periods while a smaller but significant difference was also recorded between Pre-LD vs Post-LD periods (Table S5). The reduction in the concentrations of CO could be attributed to the substantial reduction of emissions from the industrial sector during the lockdown period. The ANOVA on ranks showed that O_3 increased monotonically across the periods and with significant differences in median values. The median values of O_3 increased between Pre-LD vs During-LD (23.0–58.0) and Pre-LD vs Post-LD (23.0–72.0) (Table 2). There was a significant difference between During-LD vs Post-LD (58.0–72.0). From the Dunn's test, all of the pairwise differences were statistically significant (Table S6). Post-LD is greater than During-LD

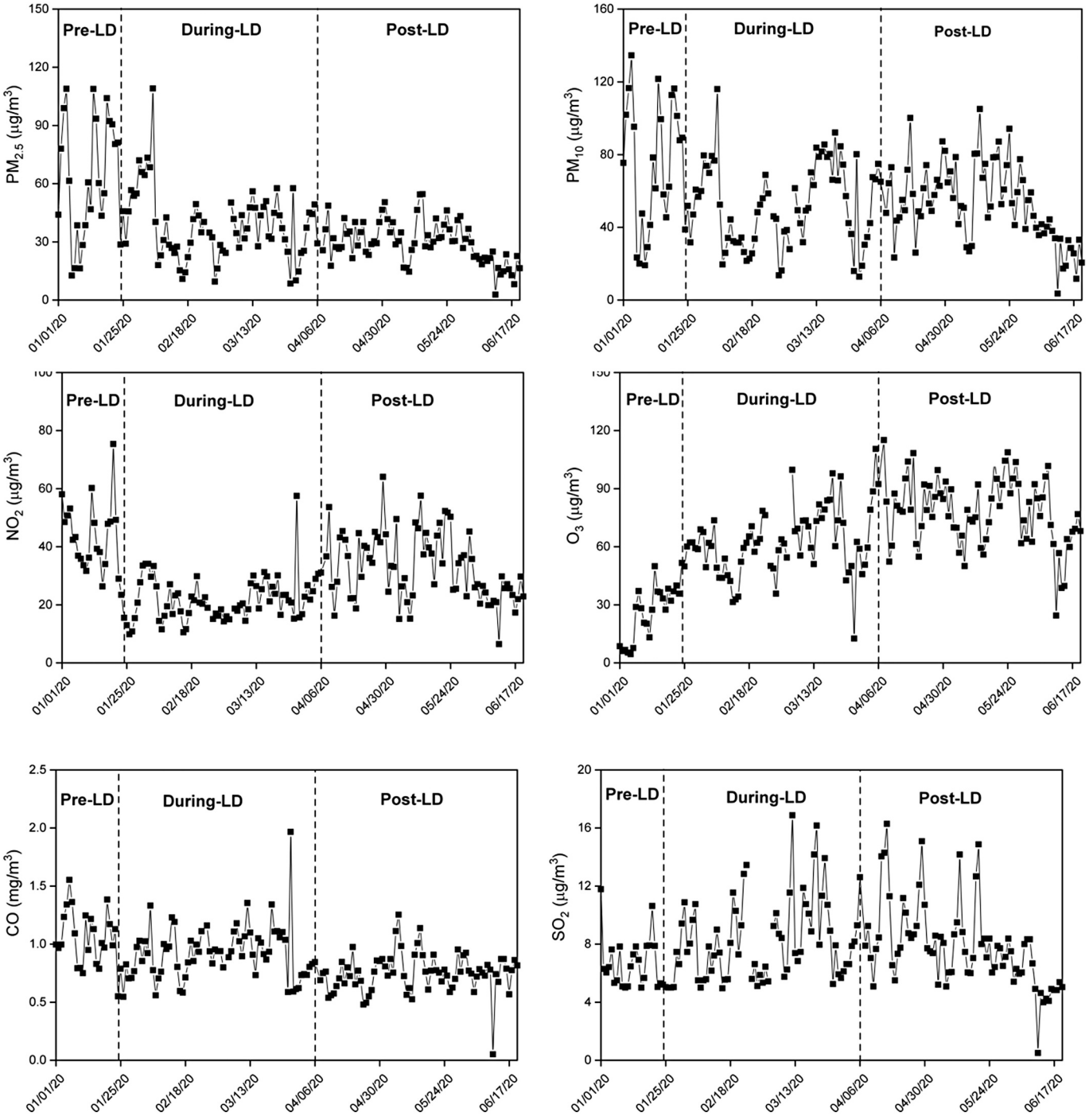

Fig. 2. Trend of 24 h average concentrations of $PM_{2.5}$, PM_{10}, NO_2, O_3, CO, and SO_2 before, during and after the 2020 lockdown period in Wuhan. The vertical lines separate the Pre-, During-, and Post-LD periods.

with difference of ranks (369), smaller compared to that of Post-LD vs Pre-LD (1711) and During-LD vs Pre-LD (1342). The increase in the concentrations of O_3 during the lockdown period may be attributed to the reduction of NOx emissions due to large reduction of vehicular traffic and operation of industrial activities which directly made the utilization of O_3 lower (titration, $NO + O_3 = NO_2 + O_2$), thereby leading to the increase in O_3 concentrations as a result of the lockdown measures (Mahato et al., 2020). There would also be an increase in ozone production through the January to June period due to increases in the photoperiods and resulting increased temperatures. Comparisons among the prior years reported below provide an accounting for the changes in photochemical activity.

The $PM_{2.5}/PM_{10}$ ratio decreased from 0.84 to 0.74 (Fig. 4) while the SO_2/NO_2 ratio increased from 0.16 to 0.37 after the lockdown was put in place (Fig. 4). The increase in the ratio of SO_2/NO_2 results from both the increase in SO_2 likely from increased coal use (Dai et al., 2019; Song et al., 2017; Wang et al., 2020) and the decrease in NOx from the reduced traffic volume. Compared to lockdown period, both $PM_{2.5}/PM_{10}$ and SO_2/NO_2 ratios reduced during the Post-LD period (Fig. 4). The continuous increase in the concentrations of NO_2, O_3, and PM_{10} immediately after the lockdown period is a strong indication that there is need to implement some control strategies to continue the reductions

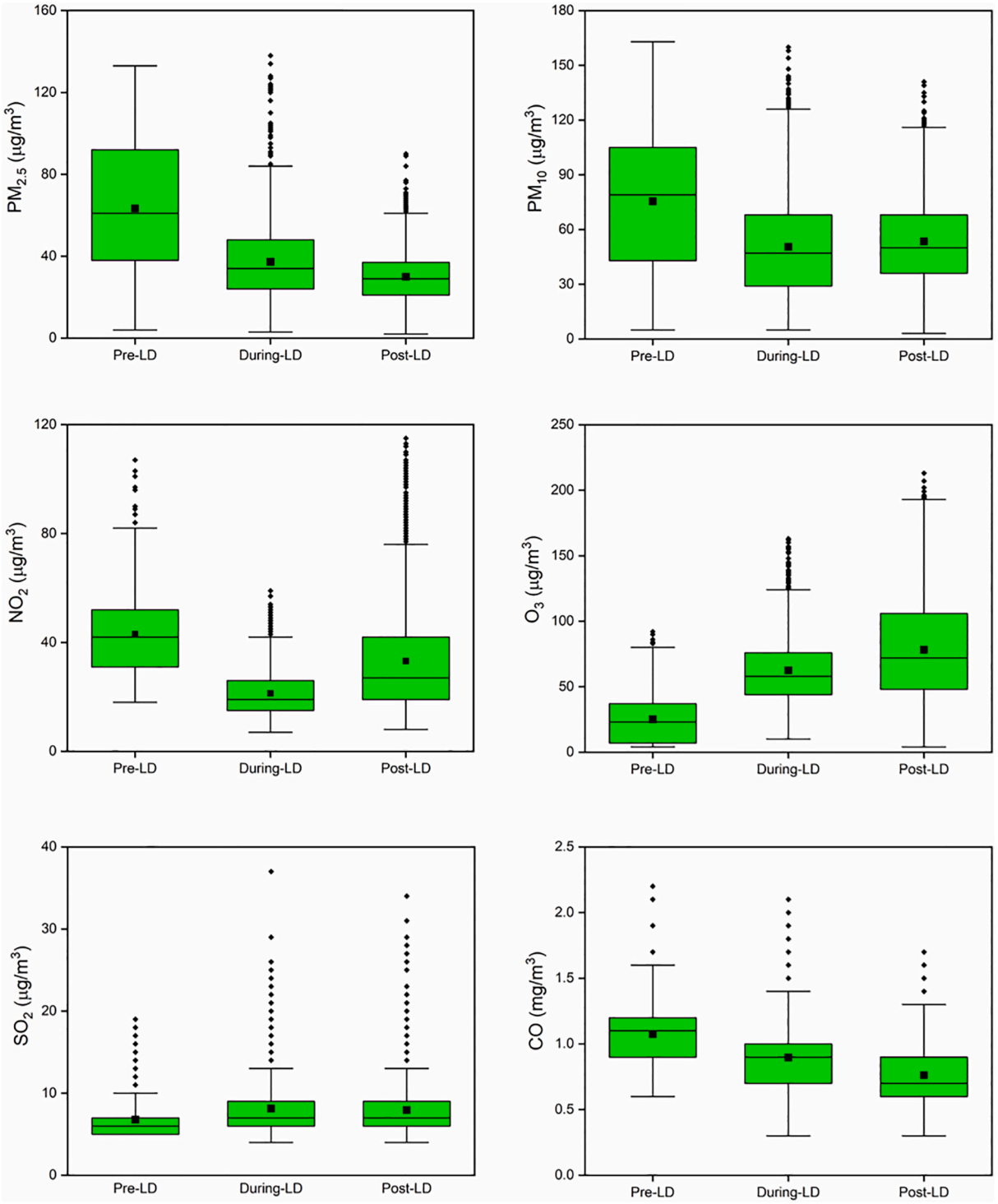

Fig. 3. Changes in concentrations of $PM_{2.5}$, PM_{10}, NO_2, O_3, SO_2, and CO before, during, and after the 2020 lockdown period in Wuhan.

in source emissions of these pollutants, otherwise, we would return to the same polluted world we had before COVID-19.

3.3. *Pollutant variations during equivalent lockdown period over the last four years*

To assess the patterns of concentrations variation of the six criteria pollutants over the last four years (2017–2020), the 1-hr concentrations of the pollutants for the same lockdown period (i.e. January 24th - April 5th) (Fig. 5) were used for the statistical analyses. Kruskal-Wallis One Way Analysis of Variance (ANOVA) on Ranks and Dunn's tests were again used. The results are summarized in Table 4 and the detailed analyses are presented in Tables S7-S12.

The median values of $PM_{2.5}$ decreased monotonically from 2017 to 2020 with substantial drops between 2017 vs 2018 (65.5–55.0), 2018 vs 2020 (55.0–34.0), and 2019 vs 2020 (53.0–34.0) (Table 5). This trend has been observed across China following the 2013 implementation of stricter controls on many emission sources (Silver et al., 2018; Lu et al., 2020b). All the pairwise differences followed this inter-annual trend. Only the differences between 2018 vs 2019 were not statistically

Table 3
Comparison of the pollutants among the three periods in 2020 using Kruskal-Wallis and Dunn's Method tests. Significant *p*-values are in **bold.**

Pollutant	Periods Tested	Test	Different?	P-value	Table
$PM_{2.5}$	All	Kruskal-Wallis	Yes	**<0.001**	S1
	Pre-During	Dunn's Method	Yes	**<0.05**	S1
	Pre-Post	Dunn's Method	Yes	**<0.05**	S1
	During-Post	Dunn's Method	Yes	**<0.05**	S1
PM_{10}	All	Kruskal-Wallis	Yes	**<0.001**	S2
	Pre-During	Dunn's Method	Yes	**<0.05**	S2
	Pre-Post	Dunn's Method	Yes	**<0.05**	S2
	During-Post	Dunn's Method	Yes	**<0.05**	S2
SO_2	All	Kruskal-Wallis	Yes	**<0.001**	S3
	Pre-During	Dunn's Method	Yes	**<0.05**	S3
	Pre-Post	Dunn's Method	Yes	**<0.05**	S3
	During-Post	Dunn's Method	No		S3
NO_2	All	Kruskal-Wallis	Yes	**<0.001**	S4
	Pre-During	Dunn's Method	Yes	**<0.05**	S4
	Pre-Post	Dunn's Method	Yes	**<0.05**	S4
	During-Post	Dunn's Method	Yes	**<0.05**	S4
CO	All	Kruskal-Wallis	Yes	**<0.001**	S5
	Pre-During	Dunn's Method	Yes	**<0.05**	S5
	Pre-Post	Dunn's Method	Yes	**<0.05**	S5
	During-Post	Dunn's Method	Yes	**<0.05**	S5
O_3	All	Kruskal-Wallis	Yes	**<0.001**	S6
	Pre-During	Dunn's Method	Yes	**<0.05**	S6
	Pre-Post	Dunn's Method	Yes	**<0.05**	S6
	During-Post	Dunn's Method	Yes	**<0.05**	S6

different. However, the largest differences were between 2020 and the other years. The largest difference in ranks was observed between 2017 vs 2020 (2173), followed by 2018 vs 2020 (1568), and 2019 vs 2020 (1550) (Table S7). These results reflect what was observed in the Kruskal-Wallis test. These showed a more substantial reduction in the $PM_{2.5}$ concentrations in 2020 during the COVID-19 lockdown period compared to the previous years when there was no lockdown.

The differences in the median values of PM_{10} for all the years were statistically significant. Similar to $PM_{2.5}$, the median values of PM_{10} declined monotonically from 2017 to 2020 with substantial reductions between 2017 vs 2020 (94.0–47.0), 2018 vs 2020 (87.0–47.0), and 2019 vs 2020 (75.0–47.0) (Table 4). The Dunn's test showed that all of the pairwise differences were also significant. The largest differences were between 2020 and the other years. The highest difference of ranks was between 2017 vs 2020 (2300), followed by 2018 vs 2020 (1870), and 2019 vs 2020 (1510) (Table S8). The substantial differences between 2020 and the previous years are indications that the concentrations of PM_{10} decreased significantly during the pandemic lockdown period in comparison to the previous years when no lockdown measures were in place.

The median values of SO_2 decreased monotonically from 2017 to 2020 with significant reductions between 2017 vs 2020 (11.0–7.0), 2017 vs 2019 (11.0–7.0), and 2017 vs 2018 (11.0–7.0) (Table 4). However, 2019 vs 2020 were indistinguishable. From the Dunn's tests, only three of the pairwise differences were statistically significant. The highest difference of ranks was recorded between 2017 vs 2020 (1316), followed by 2017 vs 2019 (1303), and 2017 vs 2018 (1180) (Table S9).

Considering the pollutant concentration trends during the lockdown period over the last four years (2017–2020), NO_2 trends were similar to PM_{10}. The differences in the median values of NO_2 over the years were statistically significant. The median values of NO_2 decreased with significant differences between 2017 vs 2020 (46.0–19.0), 2018 vs 2020 (40.0–19.0), and 2019 vs 2020 (37.5–19.0) (Table 4). The Dunn's tests also showed that all of the pairwise differences were significant with largest difference between 2017 vs 2020 (2629), followed by 2018 vs 2020 (2446), and 2019 vs 2020 (2208) (Table S10). The significant differences found between 2020 and each of the prior years indicated that NO_2 decreased substantially during the pandemic lockdown period compared to the previous years when there were no restrictions on the transportation sector. CO behaved analogously to $PM_{2.5}$. The median

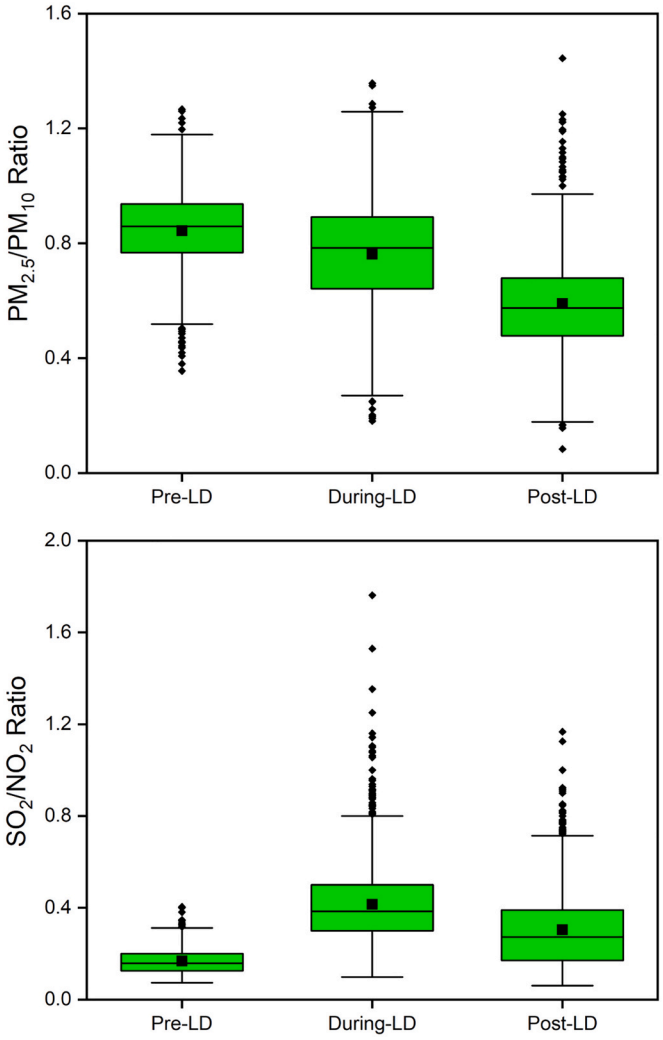

Fig. 4. $PM_{2.5}/PM_{10}$ and SO_2/NO_2 ratios before, during, and after the 2020 lockdown period in Wuhan.

values reduced monotonically over the 4 years with significant differences between 2017 vs 2020 (1.10–0.90) and 2017 vs 2018 (1.10–1.0) (Table 4). All the pairwise differences except 2018 vs 2019 were statistically significant. The highest differences in ranks were observed between 2017 vs 2020 (1636), 2017 vs 2019 (1003), and 2017 vs 2018 (863) (Table S11). In 2020, there was reduction in the concentrations of CO during the lockdown period compared to the previous years.

Contrary to the other pollutants, the Kruskal-Wallis test showed that O_3 increased monotonically with differences from one another as had been seen over the recent years (Lu et al., 2020b). There were significant differences in median values. The median values of O_3 substantially increased between 2019 vs 2020 (35.0–58.0), 2017 vs 2020 (37.0–58.0), and 2018 vs 2020 (41.0–58.0) (Table 5). Considering the pairwise differences over the years, only 2017 vs 2019 ($P = 0.284$) were not statistically different. The biggest differences were noted between 2020 and each of the other years. The largest difference in ranks was between 2020 vs 2019 (1557), followed by 2020 vs 2017 (1461), and 2020 vs 2018 (1265) (Table S12). The substantial increase in the O_3 concentrations during the 2020 lockdown period was clearly related to the NOx emissions reductions while sufficient VOCs remained available.

The maximum $PM_{2.5}$ and PM_{10} concentrations (Table 4) were observed during 2017 with maximum values of 334 μg/m^3 and 386 μg/m^3, respectively. However, the maxima were reduced to 138 μg/m^3 (58.7%) and 160 μg/m^3 (58.6%), respectively, during the same period in

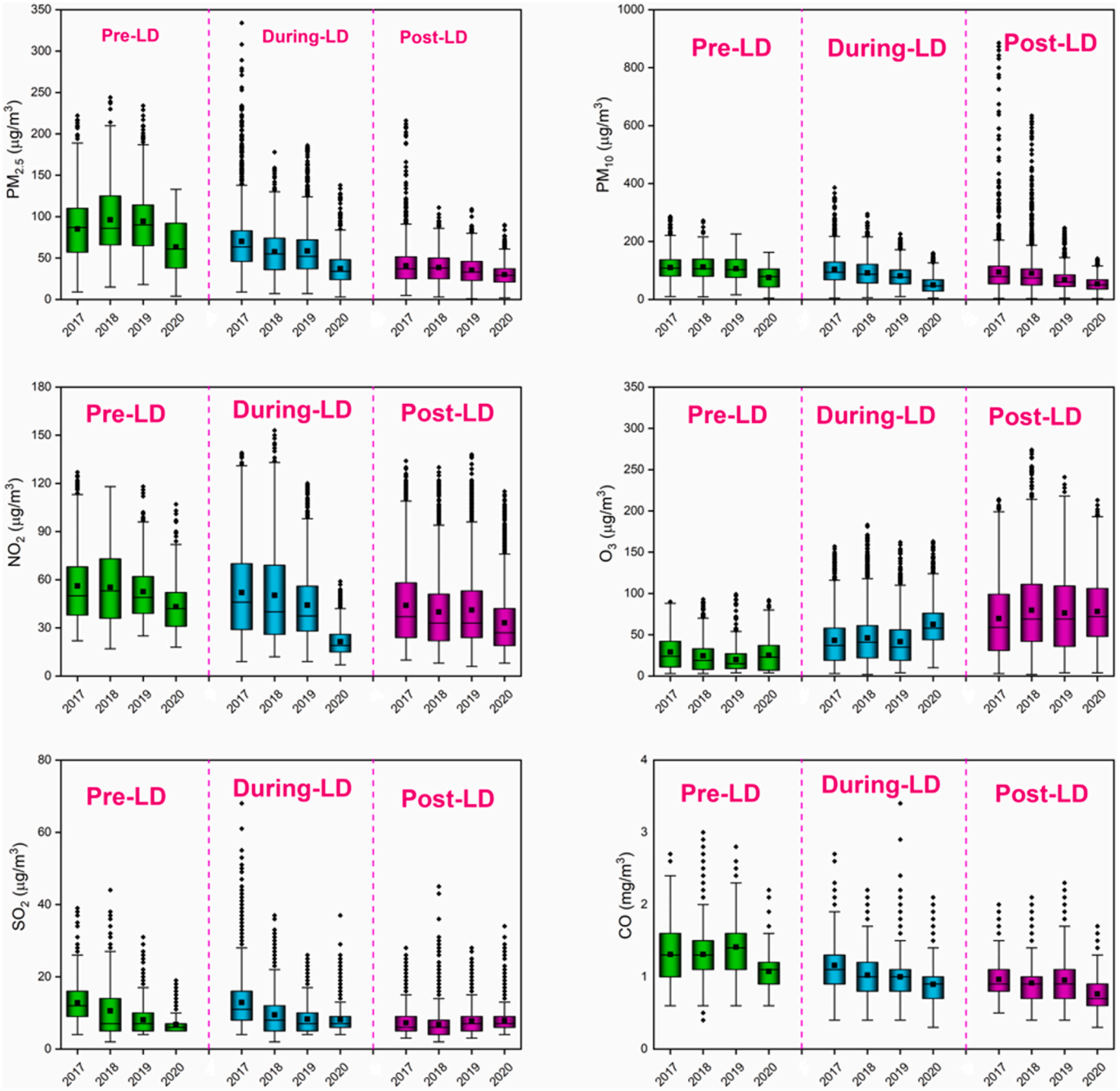

Fig. 5. Yearly changes of $PM_{2.5}$, PM_{10}, NO_2, O_3, SO_2, and CO before, during, and after the 2020 lockdown period in Wuhan.

2020. SO_2 and NO_2 had their highest concentrations measured during 2017 and 2018, respectively with values of 68 μg/m^3 and 153 μg/m^3, respectively. The lockdown measures in 2020 reduced SO_2 and NO_2 concentrations (Table 4) to 37 μg/m^3 (45.6%) and 59 μg/m^3 (61.4%), respectively. These results show that significant improvements in ambient air quality were achieved when the lockdown and related reductions in emissions were implemented. Therefore, reduced emissions will clearly lead to improved air quality in Wuhan although other measures will be required to control the ozone concentrations.

3.4. Correlation between air pollutants and meteorological variables

The correlations between the concentrations of the six criteria air pollutants and the three meteorological variables (T, WS, and RH) during the three periods of study were quantified using Pearson correlation analysis (Table 5). Prior to the lockdown period, the concentrations of $PM_{2.5}$, PM_{10}, SO_2, NO_2, and CO were positively related with temperature with PM_{10} having the highest correlation coefficient followed by $PM_{2.5}$, CO, NO_2, and SO_2. O_3, however, had negative and weak correlation with temperature. During the lockdown period, temperature was positively and strongly related to PM_{10}, SO_2, NO_2, CO, and O_3 while $PM_{2.5}$ had weak correlation with temperature. Considering the post-lockdown period, all of the species except CO had negative relationship with temperature. CO had strong correlation with WS followed by O_3. The correlation between SO_2 and WS was very weak while the remaining pollutants had negative correlations with WS before the lockdown period. During the lockdown period, only CO had moderate positive correlation with wind speed. SO_2 and PM_{10} were weakly correlated with WS while the other pollutants had negative and weaker correlation with wind speed. After the lockdown period, wind speed was

Table 4
Basic statistics for the air pollutants During-LD from 2017 to 2019.

Pollutant	Unit	Number	Mean	Std Dev.	Max	Min	Median
2017							
$PM_{2.5}$	$\mu g/m^3$	1722	70.01	38.80	334	9	63.5
PM_{10}	$\mu g/m^3$	1722	103.80	53.15	386	5	94
SO_2	$\mu g/m^3$	1722	12.87	7.87	68	4	11
NO_2	$\mu g/m^3$	1722	52.00	28.26	139	9	46
CO	mg/m^3	1722	1.16	0.33	2.7	0.4	1.1
O_3	$\mu g/m^3$	1722	43.11	31.24	157	3	37
2018							
$PM_{2.5}$	$\mu g/m^3$	1727	57.64	26.79	178	7	55
PM_{10}	$\mu g/m^3$	1727	91.46	47.19	295	6	87
SO_2	$\mu g/m^3$	1727	9.45	6.48	37	2	8
NO_2	$\mu g/m^3$	1727	50.25	29.44	153	12	40
CO	mg/m^3	1727	1.02	0.32	2.2	0.4	1
O_3	$\mu g/m^3$	1727	46.08	32.50	183	2	41
2019							
$PM_{2.5}$	$\mu g/m^3$	1772	58.61	30.76	186	7	53
PM_{10}	$\mu g/m^3$	1772	81.33	38.23	226	10	75
SO_2	$\mu g/m^3$	1772	8.29	3.92	26	4	7
NO_2	$\mu g/m^3$	1772	44.21	23.32	120	9	37.5
CO	mg/m^3	1772	1.00	0.31	3.4	0.4	1
O_3	$\mu g/m^3$	1772	41.58	29.74	162	4	35

weakly related to all air pollutants except NO_2. The relationship between RH and the air pollutants throughout the three periods were negative except CO before and after the lockdown periods. Prior to the lockdown period for instance, only SO_2 had strong negative relationship with relative humidity, weak negative correlations were observed for the other pollutants. All pollutants except CO had strong negative relationship with RH during and after the lockdown periods.

3.5. Relationships between the concentrations of pollutants and wind directions

The results of $PM_{2.5}$ and O_3 for Pre-LD, During-LD, and Post-LD periods are illustrated in Figs. 6 and 7, respectively. For Pre-LD, easterly wind gave rise to the highest $PM_{2.5}$ concentrations followed by southwesterly wind. The lowest $PM_{2.5}$ concentrations were attributed to the northerly wind. The results of PM_{10}, SO_2, NO_2, and CO with their respective wind directions are presented in Figs. S4-S7. The results of PM_{10} (Fig. S4), SO_2 (Fig. S5), NO_2 (Fig. S6) and CO (Fig. S7) were similar to that of $PM_{2.5}$ but the lowest CO concentrations were associated with the southwesterly wind. The peak values of O_3 were related to southwesterly wind followed by easterly wind while the least values were attributed to the northerly wind (Fig. 7). In the case of During-LD, the highest $PM_{2.5}$ concentrations were associated with southwesterly wind followed by easterly wind while westerly wind was responsible for the

Table 5
Results correlation coefficient analysis. Values highlighted in green indicate positive correlation, while values highlighted in yellow represent negative correlation.

Variables	Periods	$PM_{2.5}$	PM_{10}	SO_2	NO_2	CO	O_3
Temp	Pre-LD	0.553	0.656	0.371	0.443	0.502	−0.199
	During-LD	0.170	0.445	0.756	0.496	0.557	0.474
	Post-LD	−0.153	−0.129	−0.377	−0.264	0.191	−0.077
WS	Pre-LD	−0.193	−0.075	0.113	−0.119	0.575	0.391
	During-LD	−0.02	0.101	0.166	−0.035	0.345	−0.012
	Post-LD	−0.061	−0.108	0.013	−0.390	0.099	−0.011
RH	Pre-LD	−0.193	−0.211	−0.538	−0.269	0.049	−0.400
	During-LD	−0.385	−0.581	−0.594	−0.572	−0.086	−0.750
	Post-LD	−0.446	−0.630	−0.685	−0.402	0.032	−0.423

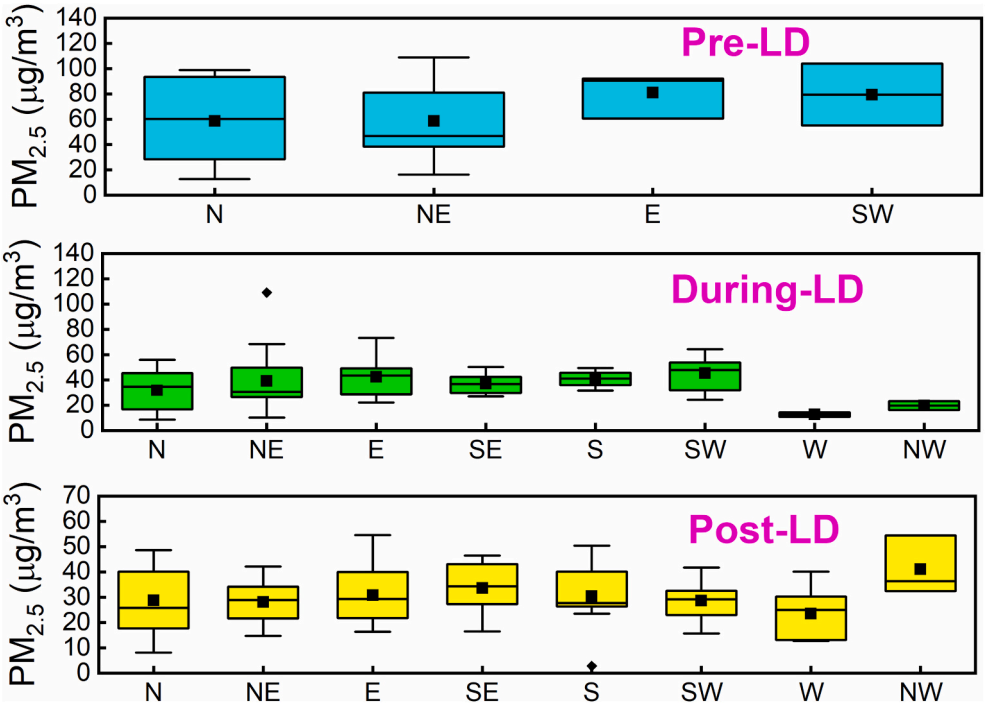

Fig. 6. Box-Whiskers plots showing the relationship between $PM_{2.5}$ concentrations and their respective wind directions during the three study periods.

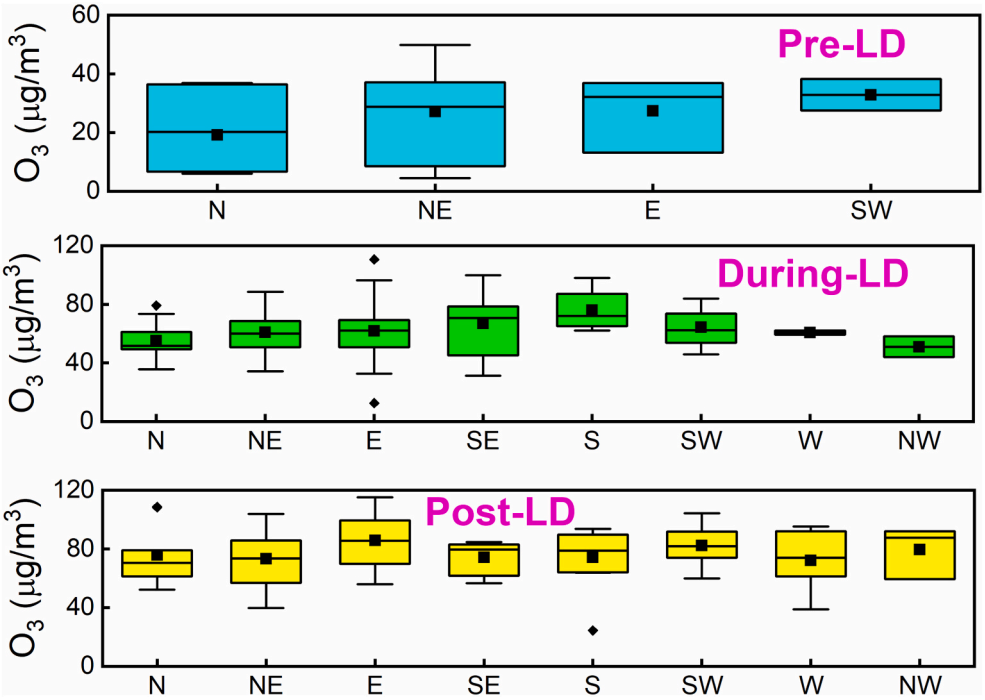

Fig. 7. Box-Whiskers plots showing the relationship between O_3 concentrations and their respective wind directions during the three study periods.

lowest $PM_{2.5}$ values. The results of PM_{10}, SO_2, and O_3 were similar as their highest concentrations were related to southerly winds (including southeast, south, and southwest winds). Northwesterly wind was responsible for the lowest concentrations of PM_{10} and O_3 while the lowest SO_2 concentrations were associated with the westerly wind. The peak values of NO_2 and CO were attributed to easterly wind followed by southeasterly wind while their lowest concentrations were related to the westerly wind. Considering the Post-LD period, the highest concentrations of $PM_{2.5}$, PM_{10}, and CO were associated with northwesterly wind while easterly wind was responsible for the peak values of SO_2, NO_2, and O_3. The least concentrations of all the pollutants were related to the westerly wind except NO_2, whose least value was attributed to the northeasterly wind.

The results revealed that air pollutants are being greatly influenced by certain wind directions compared to other directions. This could be due to two factors. Firstly, the emission of pollutants and their precursors in the up wind areas of wind from certain wind directions are larger in intensity than other areas. This leads to regional transportation of pollutants. Secondly, the lower the speed of the wind from a certain direction, the more the air pollutants accumulate.

3.6. Correlations between the air pollutants

The correlations among the six criteria air pollutants in Wuhan during the three periods in 2020 are presented in Table 6. For the Pre-LD period (January 1st-23rd, 2020), the hourly $PM_{2.5}$ concentrations were strongly correlated with hourly PM_{10} concentrations ($r^2 = 0.890$) and not correlated with the other pollutants. The hourly PM_{10} concentrations were weakly correlated with the hourly concentrations of NO_2 ($r^2 = 0.183$) and SO_2 ($r^2 = 0.084$). SO_2 was weakly correlated with NO_2 ($r^2 = 0.121$). In addition, the correlations between NO_2 and CO ($r^2 = 0.177$) and NO_2 and O_3 ($r^2 = 0.181$) were also weak.

During the lockdown period (January 24th to April 5th), the hourly $PM_{2.5}$ concentrations were strongly correlated with PM_{10} ($r^2 = 0.654$), but only weakly correlated with the other pollutants [NO_2 ($r^2 = 0.173$), CO ($r^2 = 0.248$), and SO_2 ($r^2 = 0.081$)]. The PM_{10} concentrations were weakly correlated with the concentrations of NO_2 ($r^2 = 0.184$), SO_2 ($r^2 = 0.183$), CO ($r^2 = 0.213$), and O_3 ($r^2 = 0.077$). SO_2 was weakly correlated with CO ($r^2 = 0.314$), NO_2 ($r^2 = 0.086$), and O_3 ($r^2 = 0.083$) (Table. 6). The correlation between NO_2 and CO was weak ($r^2 = 0.157$). There were very low correlations between NO_2 and O_3 and between CO and O_3.

Table 6
Correlation analysis between the air pollutants.

	$PM_{2.5}$	PM_{10}	SO_2	NO_2	CO
Pre-LD					
PM_{10}	0.890				
SO_2	0.033	0.084			
NO_2	0.079	0.183	0.121		
CO	0.029	0.068	0.057	0.177	
O_3	0.006	0.004	0.075	0.181	0.050
During-LD					
PM_{10}	0.654				
SO_2	0.081	0.183			
NO_2	0.173	0.184	0.086		
CO	0.248	0.213	0.314	0.157	
O_3	0.008	0.077	0.083	0.072	0.005
Post-LD					
PM_{10}	0.593				
SO_2	0.119	0.293			
NO_2	0.182	0.266	0.052		
CO	0.216	0.056	0.039	0.089	
O_3	0.021	0.001	0.028	0.323	0.158

Considering the Post-LD period (i.e. from April 6th to June 20th, 2020), $PM_{2.5}$ was strongly correlated with PM_{10} ($r^2 = 0.593$) but only weakly correlated with the other pollutants [NO_2 ($r^2 = 0.182$). SO_2 ($r^2 = 0.119$). CO ($r^2 = 0.216$), and O3 ($r^2 = 0.021$)] (Table. 6). The PM_{10} was weakly correlated with NO_2 ($r^2 = 0.266$), SO_2 ($r^2 = 0.293$), CO ($r^2 = 0.056$) and O_3 (0. 001). In addition, SO_2 was weakly correlated with NO_2 ($r^2 = 0.052$) and O_3 ($r^2 = 0.028$). The other correlations were also low. Thus, there is very little signal of possible sources in the interspecies correlations.

3.7. Backward trajectory analysis

In order to trace the sources as well as the transport pathways of air

masses during the three periods in 2020 (Pre-LD, During-LD and Post-LD) in Wuhan, the backward trajectories were plotted (Fig. 8). During Pre-LD period, four clusters from different wind transport directions were identified. Clusters #1 (53%) and #3 (19%) were found to dominate the transport directions as they both emanate from north, although, cluster #3 was a long-range regional transport. The duo of clusters #2 (23%) and #4 (6%) were long-range regional transport flowing from the northwest (NW) direction. Considering During-LD period, clusters #2 (56%) and #4 (15%) originated from the north and dominated the transport directions (71% in total). The remaining 29% was distributed between clusters #1 (22%) and #3 (7%), whose sources originated from the northwest (NW) and west, respectively and both were regional long-range transport. The largest share of the air masses (60%) during Post-LD period was transported from the northern direction while the remaining 40% was traced to the southwest (SW) and northwest (NW) directions. The contributions of clusters #1, #2, #3, and #4 were 48, 12, 29, and 11%, respectively. The trio of clusters #2, #3, and #4 demonstrated long-range regional transport into Wuhan.

In order to ascertain whether there exist unique transport pathways of pollutants into Wuhan, a similar trajectory analysis was carried out for the three periods in 2019 when there were no lockdown control measures in place, and the results are compared to that of 2020. During Pre-LD period of 2019 (Fig. S8), four clusters from different wind transport directions were obtained. Clusters #1 (51%) and #4 (13%) dominated the transport directions as they both originated from north while clusters #2 (17%) and #3 (18%) were coming from the northwest (NW) and west, respectively. The trio of clusters #2, #3, and #4 were found to be long-range regional transports into the study area. Considering During-LD period, clusters #2 (8%) and #3 (68%) describe the flows emanating from the north and dominated the transport directions (76% in total). Out of the remaining 25%, cluster #4 (northwest) had 16% while cluster #3 (west) had 9% and both exhibited regional long-range transport. During the Post-LD period, four clusters with two major transport pathways were also obtained. Clusters #1 (78%) and #4 (9%) dominated the transport directions and emanated from the north. Clusters #2 (10%) and #3 (3%) were approaching Wuhan from the northwest (NW) direction, and both displayed regional long-range transport.

Comparing the results of During-LD period of 2020 to 2019, 56% of the total trajectories (260) was associated with the local sources in 2020 while 68% was due to the local sources in 2019. The reduction in 2020 could be due to the control measures such as shutting down of public transport system and non-essential industries in Wuhan. Above all, there is no significant difference in the transport pathways of pollutants into Wuhan between the two years (2019 and 2020) during the three study periods as local sources dominate the sources of air pollution in Wuhan.

4. Conclusions

The impact of lockdown on air quality as a result of the COVID-19 pandemic in Wuhan was evaluated by comparing the concentrations of the six criteria air pollutants during January 1 to June 20 from 2017 to 2020. With the lockdown in place, NO_2, $PM_{2.5}$, and PM_{10} declined by 50.6, 41.2, and 33.1%, respectively, compared to Pre-LD period. The

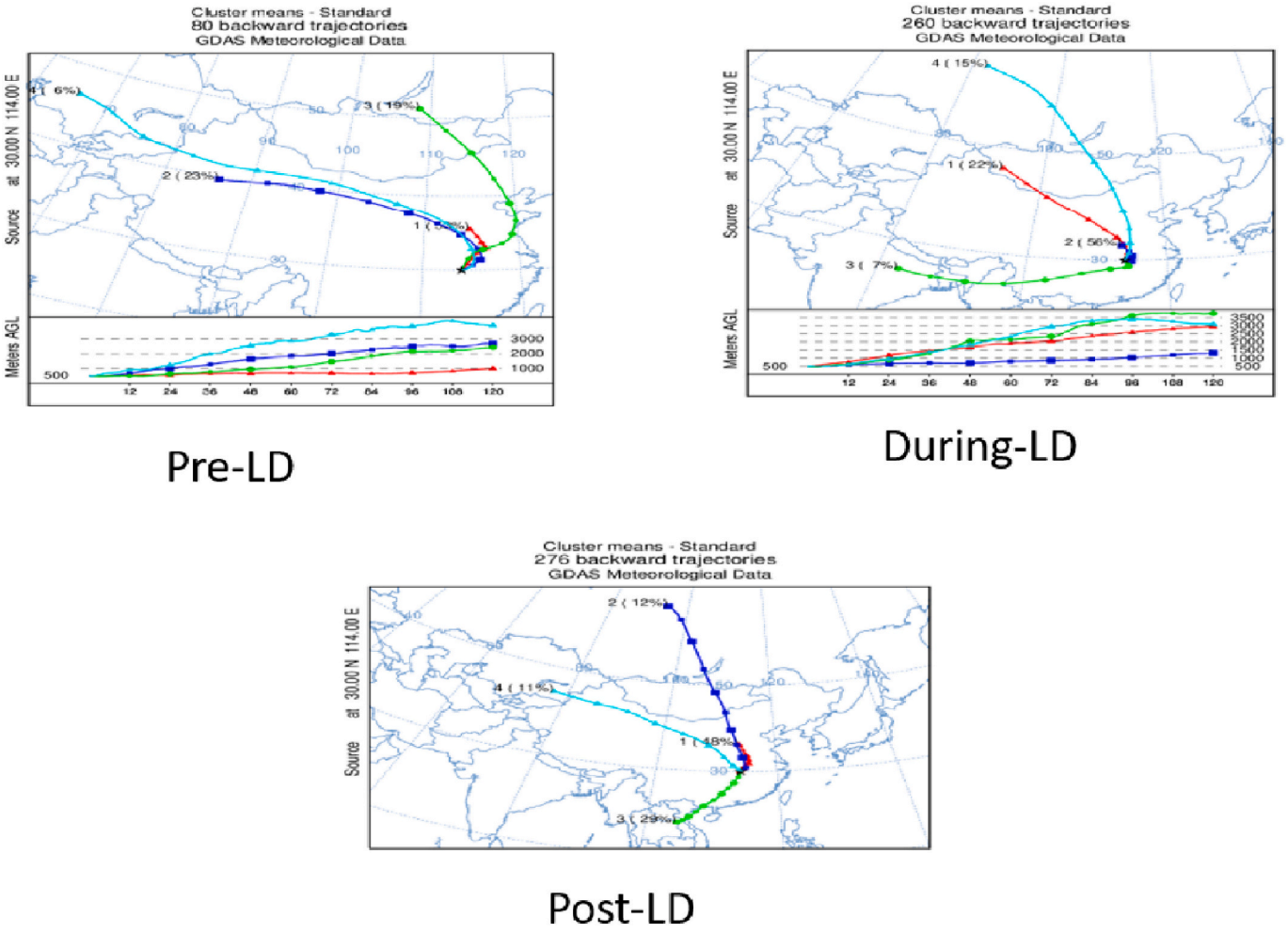

Fig. 8. Backward trajectory analysis during the three study periods in 2020.

increase in O_3 during the lockdown period while NO_2 decreased indicates that ozone in Wuhan is in a VOC-limited regime coupled with rise in photochemical activity due to increased solar radiation and temperature. However, lockdown 2020 O3 was higher than increases among prior years indicating the strong influence of the reduced NO_X emissions. Thus, the lockdown has helped to clarify the nature of ozone formation. These results suggest the need for careful investigation of VOC emissions and the potential for additional control so as to reduce the increasing ambient O_3 concentrations. Although local air quality seems largely related to local sources, transported pollutants are also important. The increase in NO_2, O_3, and PM_{10} concentrations immediately after the lockdown is a strong indication that additional control strategies must be implemented to continue to improve air quality. Otherwise, we would return to the same polluted world we had before COVID-19.

Declaration of Competing Interest

The authors declare that they have no conflict of interest.

Acknowledgements

This study was made possible with the support of CAS-TWAS President's Postgraduate Fellowship Program, the National Natural Science Foundation of China (NSFC, No. 41877310), and partly by the National Key Research and Development Program of China (No. 2016YFC0503600).

Appendix A. Supplementary data

Supplementary data to this article can be found online at https://doi.org/10.1016/j.atmosres.2020.105362.

References

Global Burden of Disease (GBD), 2020. Global age-sex-specific fertility, mortality, healthy life expectancy (HALE), and population estimates in 204 countries and territories, 1950–2019: a comprehensive demographic analysis for the Global Burden of Disease Study 2019. Lancet 396, 1135–1159.

U.S. Environmental Protection Agency (USEPA), 2019. Integrated Science Assessment (ISA) for Particulate Matter, Report No. EPA/600/R-19/188, Center for Public Health and Environmental Assessment Office of Research and Development U.S. Environmental Protection Agency Research Triangle Park, NC, December 2019.

Ayuni, N.A., Juliana, J., Ibrahim, M.H., 2014. Exposure to PM_{10} and NO_2 and Association with respiratory Health among primary School Children living near Petrochemical Industry Area at Kertih, Terengganu. Journal of Medical and Bioengineering. 3 (4), 282–287.

Brønnum-Hansen, H., Bender, A.M., Andersen, Z.J., Sørensen, J., Bønløkke, J.H., Boshuizen, H., Becker, T., Diderichsen, F., Loft, S., 2018. Assessment of impact of traffic-related air pollution on morbidity and mortality in Copenhagen municipality and the health gain of reduced exposure. Environ. Int. 121, 973–980.

Chen, H., Guo, J., Wang, C., Luo, F., Yu, X., Zhang, W., Li, J., Zhao, D., Xu, D., Gong, Q., Liao, J., Yang, H., Hou, W., Zhang, Y., 2020. Clinical characteristics and intrauterine vertical transmission potential of COVID-19 infection in nine pregnant women: a retrospective review of medical records. Lancet. https://doi.org/10.1016/S0140-6736(20)30360-3.

China State Council, 2020. The a new Coronavirus Disease (Covid-19) prevention and control. http://news.xinhuanet.com/house/bj/2014-03-17/c_126274610.htm (in Chinese).

Croft, D.P., Zhang, W., Lin, S., Thurston, S.W., Hopke, P.K., Masiol, M., Thevenet-Morrison, K., van Wijngaarden, E., Utell, M., Rich, D., 2018. The Association between respiratory Infection and Air Pollution in the setting of Air Quality Policy and Economic Change. Ann. Am. Thorac. Soc. 16, 321−−330.

Dai, Q., Schulze, B.C., Bi, X., Bui, A.A.T., Guo, F., Wallace, H.W., Sanchez, N.P., Flynn, J. H., Lefer, B.L., Feng, Y., Griffin, R.J., 2019. Seasonal differences in formation processes of oxidized organic aerosol near Houston, TX. Atmos. Chem. Phys. 19, 9641–9661.

Dunn, O.J., 1964. Multiple comparisons using rank sums. Technometrics. 6, 241–252.

He, M.Z., Kinney, P.L., Li, T.T., Chen, C., Sun, Q.H., Ban, J., Wang, J.N., Liu, S.L., Goldsmith, J., Kioumourtzoglou, M.A., 2020. Short- and intermediate-term exposure to NO2 and mortality: a multi-county analysis in China. Environ. Pollut. 261, 114165.

Hopke, P.K., Croft, D., Zhang, W., Shao, L., Masiol, M., Squizzato, S., Thurston, S.W., van Wijngaarden, E., Utell, M.J., Rich, D.Q., 2019. Changes in the acute response of respiratory disease to $PM_{2.5}$ in New York state from 2005 to 2016. Sci. Total Environ. 677, 328–339.

Statistica, 2020. Nitrogen oxide emissions volume from vehicles in China as of 2019, by vehicle type (in million tons). https://www.statista.com/statistics/1051050/china-amount-nitrogen-oxide-emission-by-type-of-vehicle/. Accessed November 5, 2020.

Hu, J., Ying, Q., Wang, Y., Zhang, H., 2015. Characterizing multi-pollutant air pollution in China: comparison of three air quality indices. Environ. Int. 84, 17–25.

Khuzestani, R.B., Schauer, J., Wei, Y., Zhang, L., Cai, T., Zhang, Y., Zhang, Y.X., 2017. Quantification of the sources of long-range transport of $PM_{2.5}$ pollution in the Ordos region, Inner Mongolia, China. Environ. Pollut. 229, 1019–1031.

Kruskal, W.H., Wallis, W.A., 1952. Use of ranks in one-criterion variance analysis. J. Am. Stat. Assoc. 47, 583–621.

Lamsal, L.N., Martin, R.V., Parrish, D.D., Krotkov, N., 2013. Scaling relationship for NO2 pollution and urban population size: a satellite perspective. Environmental Science &Technology 47, 7855–7861.

Lian, X., Huang, J., Huang, R., Liu, C., Wang, L., Zhang, T., 2020. Impact of city lockdown on the air quality of COVID-19-hit of Wuhan city. Sci. Total Environ. 742, 140556.

Lu, P., Zhang, Y.M., Lin, J.T., Xia, G.X., Zhang, W.Y., Knibbs, L.D., Morgan, G.G., Jalaludin, B., Marks, G., Abramson, M., Li, S.S., Guo, Y.M., 2020a. Multi-city study on air pollution and hospital outpatient visits for asthma in China. Environ. Pollut. 257, 113638.

Lu, X., Zhang, S., Xing, J., Wang, Y., Chen, W., Ding, D., Hao, J., 2020b. Progress of air pollution control in China and its challenges and opportunities in the ecological civilization era. Engineering. https://doi.org/10.1016/j.eng.2020.03.014.

Mahato, S., Pal, S., Ghosh, K.G., 2020. Effect of lockdown amid COVID-19 pandemic on air quality of the megacity Delhi, India. Sci. Total Environ. 730, 139086.

Muhammad, S., Long, X., Salman, M., 2020. COVID-19 pandemic and environmental pollution: a blessing in disguise? Sci. Total Environ. 728, 138820.

Pope, C.A., Dockery, D.W., 2006. Health effects of fine particulate air pollution: Lines that connect. J. Air Waste Manag. Assoc. 54, 709–742.

Sharma, S., Zhang, M., Gao, J., Zhang, H., Kota, S.H., 2020. Effect of restricted emissions during COVID-19 on air quality in India. Sci. Total Environ. 728, 138878.

Silver, B., Reddington, C., Arnold, S., Spracklen, D., 2018. Substantial changes in air pollution across China during 2015–2017. Environ. Res. Lett. 13, 114012.

Song, C., Wu, L., Xie, Y., He, J., Chen, X., Wang, T., Lin, Y., Jin, T., Wang, A., Liu, Y., Dai, Q., Liu, B., Wang, Y.N., Mao, H., 2017. Air pollution in China: status and spatiotemporal variations. Environ. Pollut. 227, 334–347.

Sulaymon, I.D., Adebayo, G.A., Sulaymon, Z.O., Oyehan, I.A., 2017. Toxicity potential of the emitted aerosols from open burning of scrap tyres. Zimbabwe. J. Sci. Technol. 12, 99–109.

Sulaymon, I.D., Jimoda, L.A., Sulaymon, Z.O., Adebayo, G.A., 2018. Assessment and toxicity potential of the gaseous pollutants emitted from laboratory-scale open burning of scrap tyres. Int. J. Environmental Engineering 9, 355–370.

Sulaymon, I.D., Mei, X., Yang, S., Chen, S., Zhang, Y., Hopke, P.K., Schauer, J.J., Zhang, Y.X., 2020. $PM_{2.5}$ in Abuja, Nigeria: Chemical characterization, source apportionment, temporal variations, transport pathways and the health risks assessment. Atmos. Res. 237, 104833.

Tiwari, S., Thomas, A., Rao, P., Chate, D.M., Soni, V.K., Singh, S., Ghude, S.D., Singh, D., Hopke, P.K., 2018. Pollution concentrations in Delhi India during winter 2015-2016: a case study of an odd-even vehicle strategy. Atmos. Poll. Res. 9 (2018), 1137–1145.

Wang, Y., Yuan, Y., Wang, Q., Liu, C., Zhi, Q., Cao, J., 2020. Changes in air quality related to the control of coronavirus in China: Implications for traffic and industrial emissions. Sci. Total Environ. 728, 138820.

WHO, 2020. WHO Coronavirus disease (COVID-19) Dashboard. https://covid19.who (Accessed November 6, 2020).

Zhang, W., Lin, S., Hopke, P.K., Thurston, S.W., van Wijngaarden, E., Croft, D., et al., 2018. Triggering of cardiovascular hospital admissions by fine particle concentrations in New York state: before, during, and after implementation of multiple environmental policies and a recession. Environ. Pollut. 242, 1404–1416.

Zhao, X., Zhou, W., Han, L., et al., 2019. Spatiotemporal variation in PM2.5 concentrations and their relationship with socioeconomic factors in China's major cities. Environ. Int. 133, 105145.

Zhao, S., Liu, S., Sun, Y., Liu, Y., Beazley, R., Hou, X., 2020. Assessing NO_2-related health effects by non-linear and linear methods on a national level. Sci. Total Environ. 744, 140909.